Discrimination of the local orientation structure of spiral Glass patterns early in human visual cortex

D.J. Mannion[*,a,b], J.S. McDonald[a], C.W.G. Clifford[a,b]

[a]*Colour, Form, and Motion Lab, School of Psychology, The University of Sydney, Australia*
[b]*Australian Research Council Centre for Excellence in Vision Science*

Abstract

The local orientation structure of a visual image is fundamental to the perception of spatial form. Reports of reliable orientation-selective modulations in the pattern of fMRI activity have demonstrated the potential for investigating the representation of orientation in the human visual cortex. Orientation-selective voxel responses could arise from anisotropies in the preferred orientations of pooled neurons due to the random sampling of the cortical surface. However, it is unclear whether orientation-selective voxel responses reflect biases in the underlying distribution of neuronal orientation preference, such as the demonstrated over-representation of radial orientations (those collinear with fixation). Here, we investigated whether stimuli balanced in their radial components could evoke orientation-selective biases in voxel activity. We attempted to discriminate the sense of spiral Glass patterns (opening anti-clockwise or clockwise), in which the local orientation structure was defined by the placement of paired dots at an orientation offset from the radial. We found that information within the spatial pattern of fMRI responses in each of V1, V2, V3, and V3A/B allowed discrimination of the spiral sense with accuracies significantly above chance. This result demonstrates that orientation-selective voxel responses can arise without the influence of a radial bias. Furthermore, the finding indicates the importance of the early visual areas in representing the local orientation structure for the perception of complex spatial form.

Key words: fMRI, V1, orientation, computational neuroimaging, spatial vision, multivariate analysis

The representation of feature orientation is fundamental to the perception of spatial form. Orientation selectivity within the human visual cortex has recently been investigated using functional magnetic resonance imaging (fMRI). Through the application of sensitive multivariate analysis methods (Haynes and Rees, 2006; Norman et al., 2006), several groups have shown that information within blood-oxygen level dependent (BOLD) signals can be used to discriminate stimulus orientation (Haynes and Rees, 2005; Kamitani and Tong, 2005; Sumner et al., 2008). These methods have revealed reliable orientation-dependent modulations in the spatial pattern of responses in the early visual regions. The orientation of a stimulus can be classified by comparing its evoked fMRI response with the established activity patterns. This classification can then be used to discriminate the stimulus from a set of possible orientations with accuracies significantly above chance.

While the capacity for accurate discrimination demonstrates that information regarding orientation is represented in the early areas of human visual cortex, the source of the orientation-selective pattern of voxel responses remains unclear. The most commonly offered explanation considers each voxel to be pooling the responses of a sample of neurons drawn from a population with a uniform distribution of preferred orientation (Boynton, 2005; Haynes and Rees, 2005; Kamitani and Tong, 2005; Sumner et al., 2008). Random variability in the spatial structure of orientation preference and voxel placement can result in subtle anisotropies in the proportion of sampled neurons preferring a given orientation, resulting in weak orientation-selectivity at the voxel level.

However, this explanation is complicated by findings which indicate that the distribution of orientation preference is not uniform across the visual field. Sasaki et al. (2006) showed that the voxels in the early visual cortex produced significantly higher BOLD responses when responding to local regions containing radial structure (those oriented towards fixation) than when containing tangential orientations. Previous investigations of orientation selectivity with fMRI have used stimuli in which the luminance of the image is modulated across the visual field to form a Cartesian grating (Haynes and Rees, 2005; Kamitani and Tong, 2005; Sumner et al., 2008). As shown in Figure 1, a given stimulus of this type contains regions that differ in the degree of radial orientation structure and the retinotopic location of such regions varies with stimulus orientation. The existence of a radial bias suggests that the demonstrated capacity for orientation discrimination may be driven by differences in the spatial distribution of radial structure across the stimulus set.

Evidence regarding the influence of a bias towards radial orientations has, however, been mixed. Haynes and Rees (2005) found no preference for stimulus quadrants containing radial orientations compared with those containing tangential. Kamitani and Tong (2005) and Sumner et al. (2008) reported the presence of a weak radial bias, though further analyses by Kamitani

---

[*]Corresponding author
Email address: `damienm@psych.usyd.edu.au` (D.J. Mannion)
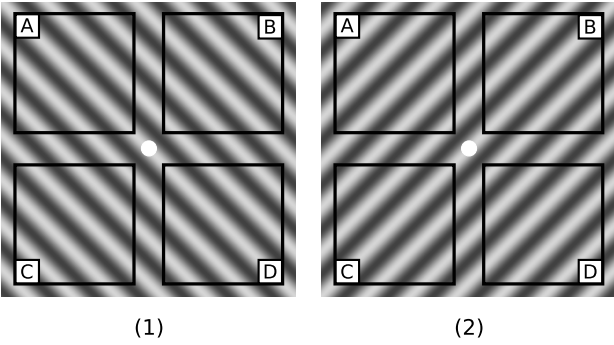
Figure 1: Illustration of the local orientation structure of oblique Cartesian gratings. For a centrally fixating observer, the regions A and D in stimulus 1 (1A and 1D) contain predominantly radial orientations while those in 1B and 1C are predominantly tangential. The opposite configuration is observed in an orthogonal grating (stimulus 2), in which 2A and 2D are predominantly tangential while 2B and 2C are predominantly radial.

and Tong (2005) designed to reduce the influence of the radial preference suggested that it did not contribute substantially to the discrimination accuracy.

Here, we investigated whether the effect of a radial bias was required for orientation discrimination from fMRI signals by using stimuli that were balanced in their radial components — spirals. In such stimuli, the local orientation structure is defined by an angular displacement relative to the radial orientation, with greater displacements increasing the pitch of the spiral and the sign of displacement determining the spiral's sense (opening clockwise or anti-clockwise). By attempting to discriminate the sense of a spiral of ±45° pitch, we ensured that the local comparison was always between orthogonal orientations with an equal angular displacement from the radial. This stimulus configuration was also balanced in the local offset from cardinal orientations (horizontal and vertical), controlling for the bias of the oblique effect (Furmanski and Engel, 2000).

We instantiated the spiral form in textures defined by randomly placed dot pairings (dipoles). Such Glass patterns (Glass, 1969) are created by positioning the elements of each dipole at a relative orientation that is consistent with the desired global form. Neurophysiological (Smith et al., 2002, 2007) and computational modeling (Wilson and Wilkinson, 1998) studies have suggested that the early visual regions are capable of recovering this local orientation structure from the noisy and ambiguous signals given by the dot pairings. Here, we used spiral Glass patterns to investigate the potential for accurate discrimination of the orientation structure underlying such complex spatial form.

Materials and Methods

Subjects

Five experienced psychophysical observers with normal or corrected-to-normal vision participated in the current study. Subjects gave their informed consent and the protocol was approved by a local ethics committee.

Apparatus

A Philips 3T scanner with a whole-head coil was used to conduct the MRI. Anatomical images were collected using a turbo field-echo protocol for enhanced grey-white contrast, and consisted of whole-head scans in the axial and sagittal planes (voxel size = 1mm isotropic) and a high-resolution partial-head coronal scan (voxel size = 0.75mm isotropic) to recover maximum detail in the occipital lobes. Functional images were collected using a T_2^* sensitive, boustrophedon, field-echo echo-planar imaging pulse sequence (TR = 3s, TE = 30ms, flip angle = 90°, FOV = 70.5 × 192 × 192mm, matrix = 128 × 128, voxel size = 1.5mm isotropic). Images were acquired in 47 ascending interleaved slices in the coronal plane covering the occipital lobes.

Stimuli were displayed on a Philips LCD monitor with a display resolution of 1024 × 768 pixels that was positioned behind the bore. Subjects viewed the monitor from a distance of 158cm via a mirror mounted on the headcoil, resulting in a viewing angle of 12.6° × 9.5°.

Stimuli were presented using PsychToolbox 3.0.8 (Brainard, 1997; Pelli, 1997). Behavioural responses were indicated via a LU400-PAIR Lumina response pad (Cedrus Corporation, San Pedro, CA, USA). Except where otherwise specified, analyses were performed using SPM5 (http://www.fil.ion.ucl.ac.uk/spm) on Matlab 7.5 and custom routines on Python 2.5.

Stimuli

The construction of each Glass pattern began by assigning a random position in the image as the base for each dipole, based on a uniform allocation over area. Dot pairs were then placed equidistant from each base with an inter-dot distance of 0.12° Spiral patterns opening anti-clockwise / clockwise were formed by placing the dots at an angle of +45° / −45° relative to the radial angle, as shown in Figure 2. Each dot had a Gaussian profile (σ = 0.019°) and each dot pair was randomly assigned to be either a 100% contrast increment or decrement from the 37 cd/m² background, with the paired dots always having the same polarity. The overall dot density was approximately 45 dots / deg², resulting in a given dot having an average of 2.0 dots closer than its partner. The stimuli were presented in a circular aperture with an inner radius of 1.2° and an outer radius of radius 4.3°.
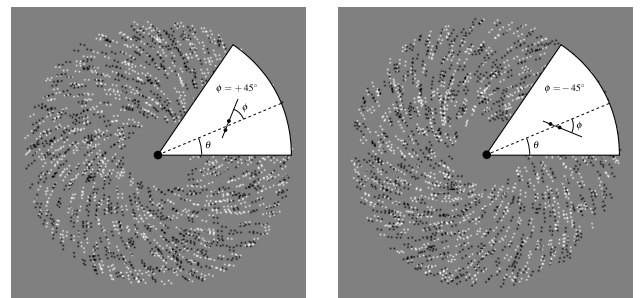
Figure 2: Example anti-clockwise (left) and clockwise (right) spiral Glass patterns. Each dot pair is oriented at an angle (ϕ) of +45° (anti-clockwise) or -45° (clockwise) relative to the radial angle (θ).

Design

Subjects observed 10 runs of 270s duration (90 volumes) of the experiment protocol, with each run consisting of 18 blocks. Each block was 15s in duration and contained either clockwise or anti-clockwise Glass patterns. The blocks alternated over the course of the run, and the initial block was counterbalanced between clockwise and anti-clockwise over the 10 runs. A new Glass pattern instance was presented every second within each block. See Supplementary Movie for an example of the stimulus presentation protocol.

During the same scanning session, subjects observed two runs of 255s duration (85 volumes) of the stimulus localiser protocol. Each run consisted of 17 blocks of 15s duration, and began with a block of fixation followed by alternating blocks of Glass patterns and incoherent patterns, interleaved with blocks of fixation. The stimuli alternated between clockwise and anti-clockwise spirals on successive Glass pattern blocks.

During all the runs, subjects performed an attentionally demanding dimming task in which they responded to increments and decrements in the luminance of the central fixation circle.

fMRI acquisition and pre-processing

A mean anatomical image was formed for each subject by combining the axial and sagittal whole-head scans and the coronal partial-head scan. Before averaging, each anatomical image was inhomogeneity corrected (Manjòn et al., 2007), coregistered, and resampled to a voxel resolution of 0.75mm (isotropic) where necessary. Each subject's mean anatomical was then segmented using the automatic routines of mrGray (Teo et al., 1997) and ITKGray (Yushkevich et al., 2006, http://white.stanford.edu/software) followed by careful hand editing.

Functional images were corrected for differences in slice timing with reference to the middle slice. Between and within run subject movement was estimated and corrected by applying the movement parameters and reslicing using 4th degree B-spline interpolation. The images were also placed into register with the world space of the subject's mean anatomical by applying coregistration parameters to each image's affine transformation matrix.

Region of interest (ROI) definition

In a separate scanning session, subjects completed standard protocols for defining the early retinotopic regions of visual cortex. The functional data from this session were transformed onto a flattened representation of the cortical surface using mrVista (http://white.stanford.edu/software) to aid in the delineation of the borders between visual areas. We used the nomenclature and criteria of Wandell et al. (2007) to manually define areas V1, V2, V3, V3A/B, and hV4 based on the phase of the responses of each voxel to standard polar angle (wedge) and eccentricity (ring) scans (Engel et al., 1997).

The mask defining each retinotopic area was transformed from the flat-map into the space of the subject's anatomical, smoothed (FWHM = 1.5mm), and resliced to the resolution of the functional images using 4th degree B-spline interpolation.

The voxels within each ROI contained a mask value that reflected the cumulative influence of such transformations. To prevent overlapping voxels between adjacent ROIs, each voxel was assigned to the ROI for which it possessed the greatest mask value.

Analysis

The localiser runs were modelled as boxcar functions for the periods of stimulation associated with each of the three conditions (clockwise Glass, anti-clockwise Glass, incoherent) and analysed with the general linear model as implemented in SPM5. The parameters derived from the estimation of subject movement were included as covariates of no interest in the model. High-pass filtering (cutoff = 128s) and a correction for autocorrelation using an AR(1) method were applied.

Analysis of the experimental runs began by shifting the timecourse of each run by +2 volumes (6s) to compensate for the lag in the haemodynamic response. The volumes corresponding to the first and last blocks of each run were subsequently removed from analysis. The signal timecourse of each voxel was then high-pass filtered (cutoff = 128s) and normalised (z-scored) within the remaining volumes of each run. Response vectors were then formed by averaging the signal evoked during each block (five volumes) for each voxel.

The pattern analysis was conducted separately for each ROI, and was implemented using a 10-fold leave-one-out strategy in which the responses from a given run (in turn) were designated to form the test set while those from the remaining runs formed the training set. This approach yielded 16 items in the test set and 144 items in the training set, with each split equally into clockwise and anti-clockwise examples. The training set was submitted to the linear support vector machine algorithm as implemented in SVM^{Light} (Joachims, 1998) to determine the optimal hyperplane for discrimination of the clockwise and anti-clockwise examples.

This yielded a weighting for each voxel included in the training set that reflected a bias in the responses of the voxel towards clockwise or anti-clockwise Glass stimuli. This model was then applied to the test set (which, as outlined above, was not used in deriving the model parameters) to produce a classification for each test example as either clockwise or anti-clockwise. The accuracy of such classification was taken as the mean percentage correct over the 10 iterations of the leave-one-out procedure.

To optimise the analysis, we implemented a feature selection strategy aimed at restricting the included voxels to those that displayed the greatest response to stimulation (Mitchell et al., 2004). The voxels were ranked in descending order by the t value from the all conditions (clockwise Glass, anti-clockwise Glass, incoherent) > fixation contrast obtained from the separate localiser runs. The pattern analysis was performed iteratively by including additional voxels when forming the data sets, with the first iteration undertaken with the top five voxels and continuing with a step size of five voxels until n, where n was the number of voxels at which the ranked t value fell below significance ($p < .05$, uncorrected) for the ROI under analysis.

The variation in classifier accuracy with an increasing number of voxels was fitted by an exponential growth function of the form

$$y = 0.5 + (B - 0.5)(1 - e^{(-x/N)}) \qquad (1)$$

where y is the classification accuracy, B is the asymptote, x is the number of included voxels, and N the exponential growth constant in units of number of voxels. The fitted asymptote value was interpreted as the accuracy of the ROI in discriminating between clockwise and anti-clockwise Glass patterns. In cases where the classifier accuracy did not conform to an exponential growth function, the mean accuracy over the range of voxels included was taken as the accuracy of the ROI. As shown in Supplementary Figure 1, taking the fitted asymptote rather than the mean over the range of voxels does not substantially affect the estimates of classification accuracy.

The statistical significance of the classification accuracy of each region was evaluated via a one-sample t-test of the asymptotic accuracy across subjects against a chance population mean of 50%.

Results and Discussion

We investigated whether the spatial pattern of fMRI signals in the early visual areas contained information that would allow discrimination of clockwise and anti-clockwise spiral Glass stimuli. For each subject, we used a multivariate classification method to obtain measures of discrimination accuracy for each of the early visual areas. As shown in Figure 3, the mean accuracy was above 50% as early as V1 (see Supplementary Figure 1 for single subject results). This performance was significantly above chance in V1, $t(4) = 3.72, p = 0.010$; V2, $t(4) = 5.01, p = 0.003$; V3, $t(4) = 3.76, p = 0.010$; and V3A/B, $t(4) = 3.30, p = 0.015$; the difference was not significant in hV4, $t(4) = 1.21, p = 0.146$ (all ps one-tailed). Permutation analysis demonstrated that the mean discrimination accuracy was approximately 50% (chance) in all areas when the labels of the items in the training set were assigned randomly (shuffled), as shown in Supplementary Figure 2.

Discrimination of spiral sense (anti-clockwise or clockwise) required the comparison of local regions that were balanced in their radial components. The spiral sense was determined by the sign of the angular offset of the local orientations from the radial, with the magnitude of displacement matched in anti-clockwise and clockwise spirals. This stimulus construction allowed us to test the possibility that previous reports of orientation discrimination using fMRI (Haynes and Rees, 2005; Kamitani and Tong, 2005; Sumner et al., 2008) were driven by differences in local radial structure. The significant accuracy in discriminating anti-clockwise and clockwise spirals demonstrated here indicates that the influence of a radial bias is not necessary for the discrimination of stimulus orientation on the basis of fMRI activity patterns.

The presence of voxel level orientation selectivity has been attributed to anisotropies in the sampled distribution of neuronal orientation preference (Boynton, 2005; Haynes and Rees,
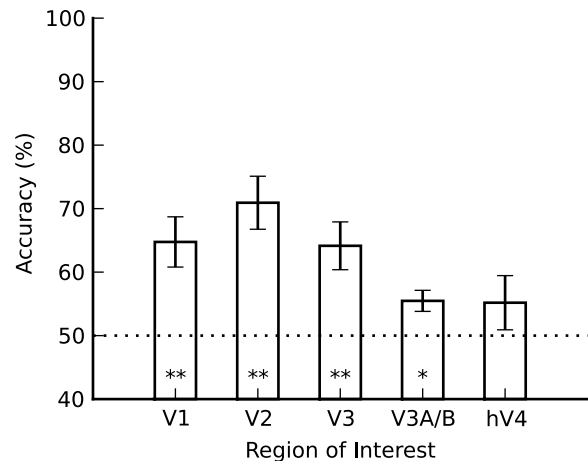
Figure 3: Mean classification accuracy across observers for each region of interest. Error bars represent SEM across the five subjects. Asterisks indicate significance on a one-sample t-test (* $p < .05$; ** $p \leq .01$; one-tailed)

2005; Kamitani and Tong, 2005; Sumner et al., 2008). Simulated maps of neuronal orientation preference across the cortical surface, in which each neuron's preferred orientation is determined from a uniform distribution of orientations, have shown that biases in the pooled orientation response can emerge when the map is sampled at the size of typical fMRI voxels (Boynton, 2005; Haynes and Rees, 2005; Kamitani and Tong, 2005). However, the distribution of neuronal orientation preference in human visual cortex appears to be non-uniform, with fMRI and behavioural evidence suggesting an over-representation of radial orientations (Sasaki et al., 2006). The results of this study suggest that random sampling can produce reliable biases for non-radial orientations in the presence of such an anisotropic distribution of neuronal orientation preference.

The discrimination of anti-clockwise and clockwise spiral Glass patterns in the current study required the recovery of local orientation structure from the cues given by the relative positions of paired dots. Random local orientation information was introduced by the presence of neighboring non-partner dots, subjecting the orientation structure to considerable ambiguity and noise. The observed discrimination accuracy in the early regions of visual cortex demonstrates the robustness of the local orientation extraction process. This is consistent with previous neurophysiological investigations in the macaque, which showed that orientation-selective neurons within V1 (Smith et al., 2002) and V2 (Smith et al., 2007) responded reliably to Glass pattern dipoles presented within their receptive fields. Such a representation of the local orientation structure can then provide input for higher level processes which pool over space to generate selectivity for complex spatial form (Ostwald et al., 2008; Wilson and Wilkinson, 1998).

Acknowledgments

References

Boynton, G. M., 2005. Imaging orientation selectivity: decoding conscious perception in V1. Nat. Neurosci. 8 (5), 541–542.

Brainard, D. H., 1997. The psychophysics toolbox. Spat. Vis. 10 (4), 433–436.

Engel, S. A., Glover, G. H., Wandell, B. A., 1997. Retinotopic organization in human visual cortex and the spatial precision of functional MRI. Cereb. Cortex 7 (2), 181–192.

Furmanski, C. S., Engel, S. A., 2000. An oblique effect in human primary visual cortex. Nat. Neurosci. 3 (6), 535–536.

Glass, L., 1969. Moiré effect from random dots. Nature 223 (5206), 578–580.

Haynes, J.-D., Rees, G., 2005. Predicting the orientation of invisible stimuli from activity in human primary visual cortex. Nat. Neurosci. 8 (5), 686–691.

Haynes, J.-D., Rees, G., 2006. Decoding mental states from brain activity in humans. Nat. Rev. Neurosci. 7 (7), 523–534.

Joachims, T., 1998. Making large-scale support vector machine learning practical. In: Schölkopf, B., Burges, C., Smola, A. (Eds.), Advances in Kernel Methods: Support Vector Machines. MIT Press, Cambridge, MA.

Kamitani, Y., Tong, F., 2005. Decoding the visual and subjective contents of the human brain. Nat. Neurosci. 8 (5), 679–685.

Manjòn, J. V., Lull, J. J., Carbonell-Caballero, J., Garca-Martì, G., Martì-Bonmatì, L., Robles, M., 2007. A nonparametric MRI inhomogeneity correction method. Med. Image. Anal. 11 (4), 336–345.

Mitchell, T. M., Hutchinson, R., Niculescu, R. S., Pereira, F., Wang, X., Just, M., Newman, S., 2004. Learning to decode cognitive states from brain images. Machine Learning 57 (1), 145–175.

Norman, K. A., Polyn, S. M., Detre, G. J., Haxby, J. V., 2006. Beyond mind-reading: multi-voxel pattern analysis of fMRI data. Trends Cogn. Sci. 10 (9), 424–430.

Ostwald, D., Lam, J. M., Li, S., Kourtzi, Z., 2008. Neural coding of global form in the human visual cortex. J Neurophysiol 99 (5), 2456–2469.

Pelli, D. G., 1997. The videotoolbox software for visual psychophysics: transforming numbers into movies. Spat. Vis. 10 (4), 437–442.

Sasaki, Y., Rajimehr, R., Kim, B. W., Ekstrom, L. B., Vanduffel, W., Tootell, R. B. H., 2006. The radial bias: a different slant on visual orientation sensitivity in human and nonhuman primates. Neuron 51 (5), 661–670.

Smith, M. A., Bair, W., Movshon, J. A., 2002. Signals in macaque striate cortical neurons that support the perception of Glass patterns. J. Neurosci. 22 (18), 8334–8345.

Smith, M. A., Kohn, A., Movshon, J. A., 2007. Glass pattern responses in macaque V2 neurons. J. Vis. 7 (3), 1–15.

Sumner, P., Anderson, E. J., Sylvester, R., Haynes, J.-D., Rees, G., 2008. Combined orientation and colour information in human V1 for both L-M and S-cone chromatic axes. Neuroimage 39 (2), 814–824.

Teo, P. C., Sapiro, G., Wandell, B. A., 1997. Creating connected representations of cortical gray matter for functional MRI visualization. IEEE Trans Med Imaging 16 (6), 852–863.

Wandell, B. A., Dumoulin, S. O., Brewer, A. A., 2007. Visual field maps in human cortex. Neuron 56 (2), 366–383.

Wilson, H. R., Wilkinson, F., 1998. Detection of global structure in Glass patterns: implications for form vision. Vision Res. 38 (19), 2933–2947.

Yushkevich, P. A., Piven, J., Hazlett, H. C., Smith, R. G., Ho, S., Gee, J. C., Gerig, G., 2006. User-guided 3D active contour segmentation of anatomical structures: significantly improved efficiency and reliability. Neuroimage 31 (3), 1116–1128.